VIII International Conference on Computational Plasticity
COMPLAS VIII
E. Oñate and D. R. J. Owen (Eds)

3D FRACTURE ANALYSIS OF CONCRETE UNDER UNIAXIAL TENSION AND COMPRESSION SOLICITATION

A. Caballero, I. Carol and C. M. López

School of Civil Engineering (ETSECCPB)
Technical University of Catalonia (UPC)
E-08034 Barcelona, Spain
e-mail: antonio.caballero@upc.edu; ignacio.carol@upc.edu; carlos.maria.lopez@upc.edu

1 INTRODUCTION

A numerical approach for the 3D meso-mechanical analysis of heterogeneous materials using zero-thickness join/interface elements with constitutive laws based on non-linear fracture mechanics has been developed. The approach is based on a polyhedron representation of the larger aggregate pieces, which are embedded in a matrix phase representing mortar plus the smaller aggregates. The polyhedric geometry is numerically generated by standard Voronoï/Delaunay tessellation. The main peculiarity of the approach is that the continuum elements thus obtained are all assumed to behave linear elastic. The non-linearity and failure capability of the model is achieved by means of zero-thickness interface elements equipped with a non-linear fracture-based law, which are inserted between all particle-matrix interfaces and also along selected matrix-matrix inter-element boundaries representing the main potential crack patterns. The procedure presented is an extension of previous work in the same group, concerning 2D meso-mechanical analysis of concrete specimen[1].

2 INTERFACE CONSTITUTIVE LAW

The 3D constitutive law is an extension and modification of the 2D formulation used in previous works[2]. In a local orthogonal reference system, the behavior of the joints is formulated in terms of one normal and two tangential traction components on the plane of the joint, $\sigma = [\sigma_N, \sigma_{T1}, \sigma_{T2}]^t$ and the corresponding relative displacements $u = [u_N, u_{T1}, u_{T2}]^t$. The constitutive formulation conforms to work-softening elasto-plasticity, in which plastic relative displacements can be identified with crack openings.

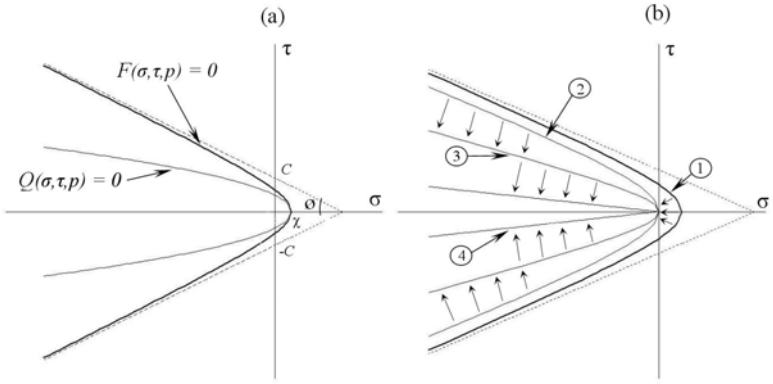

Fig. 1. Interface cracking laws: fracture surface and plastic potential (left); evolution of fracture surface (right).

The initial loading (failure) surface F = 0 is given as three-parameter hyperboloid (tensile strength χ, asymptotic "cohesion" C, and asymptotic friction angle tanϕ). These three parameters, that are defined by means of some softening laws and govern the yield surface evolution, are as well functions of one single history variable which is the work consumed in fracture processes, W^{cr}. To control the process of evolution of F, the model has two parameters that represent the classic energy of fracture in Mode I, G_F^I (pure tension) and a second energy under "Mode IIa" defined under shear and high compression, G_F^{IIa}, with values generally higher than its mode I counterpart. When cracking starts, the loading surface begins to shrink, and if pure tension is applied, the loading surface shrinks and moves to become another hyperboloid with vertex at the coordinate origin. However, if shear-compression is applied, the hyperboloid degenerates becoming a cone that represents the residual friction after all roughness of the crack surface has been eliminated.

3 APPLICATION EXAMPLE: 14-AGGREGATE CUBICAL SPECIMEN

Due to the dramatic increase of degrees of freedom, the specimen considered for this calculation is one of the simplest possible which could be still considered in a broad sense representative of the overall concrete behavior. The specimen contains 14 aggregates, and even if very simple, the resulting mesh with interfaces has 6254 nodes, 5755 tetrahedra and 3991 interface elements. The material parameters used are: E = 70000 MPa (aggregate), E = 25000 MPa (mortar) and ν = 0.20 (both) for the continuum elements; for the aggregate-mortar interfaces: $K_N = K_T = 10^9$ MPa/m, tangϕ_0 = 0.8, tangϕ_r = 0.2, tensile strength χ_0 = 2 MPa, C_0 = 7.0 MPa, G_f^I = 0.03 N/mm, G_f^{IIa} = 10 G_f^I; for the mortar-mortar interfaces the same parameters except for χ_0 = 4 MPa, c_0 = 14.0 MPa, G_f^I = 0.06 N/mm. Two loading cases are considered for this specimen, uniaxial tension and compression.

3.1 Results in uniaxial tension

A prescribed tensile displacement is applied to the upper side of the specimen, while the lower side is fixed vertically. Lateral displacements are left free, except for two nodes at the base of specimen to prevent rigid-body motion/rotation. The resulting average stress-strain curve is represented in the lower-left diagram of figure 2, in which average strain is calculated as the prescribed displacement divided by specimen length, and average strain as the sum of reactions, divided by the area surface. The sequence of cracking and deformed mesh for loading states A_t, B_t, C_t together with the magnified deformed shapes of the specimen are also shown in figure 2 (upper-left). The images in the left column depict only the interfaces which have exceeded the initial strength and are in "plastic loading" situation. Those pictures appear with different color intensities depending on the amount of energy dissipated in fracture, W^{cr}. In the figure, it can be clearly seen that initially (loading stage A) cracked interfaces are spread more or less uniformly over the specimen. Progressively, row B_t, fracture advances faster in some interfaces, while more and more interfaces start unloading and, therefore, they disappear from the figure. Finally, in row C_t, only one single surface remains active, which represents the final macro crack splitting the specimen in two pieces. Note the complexity of crack patterns that emerge from this simple geometry.

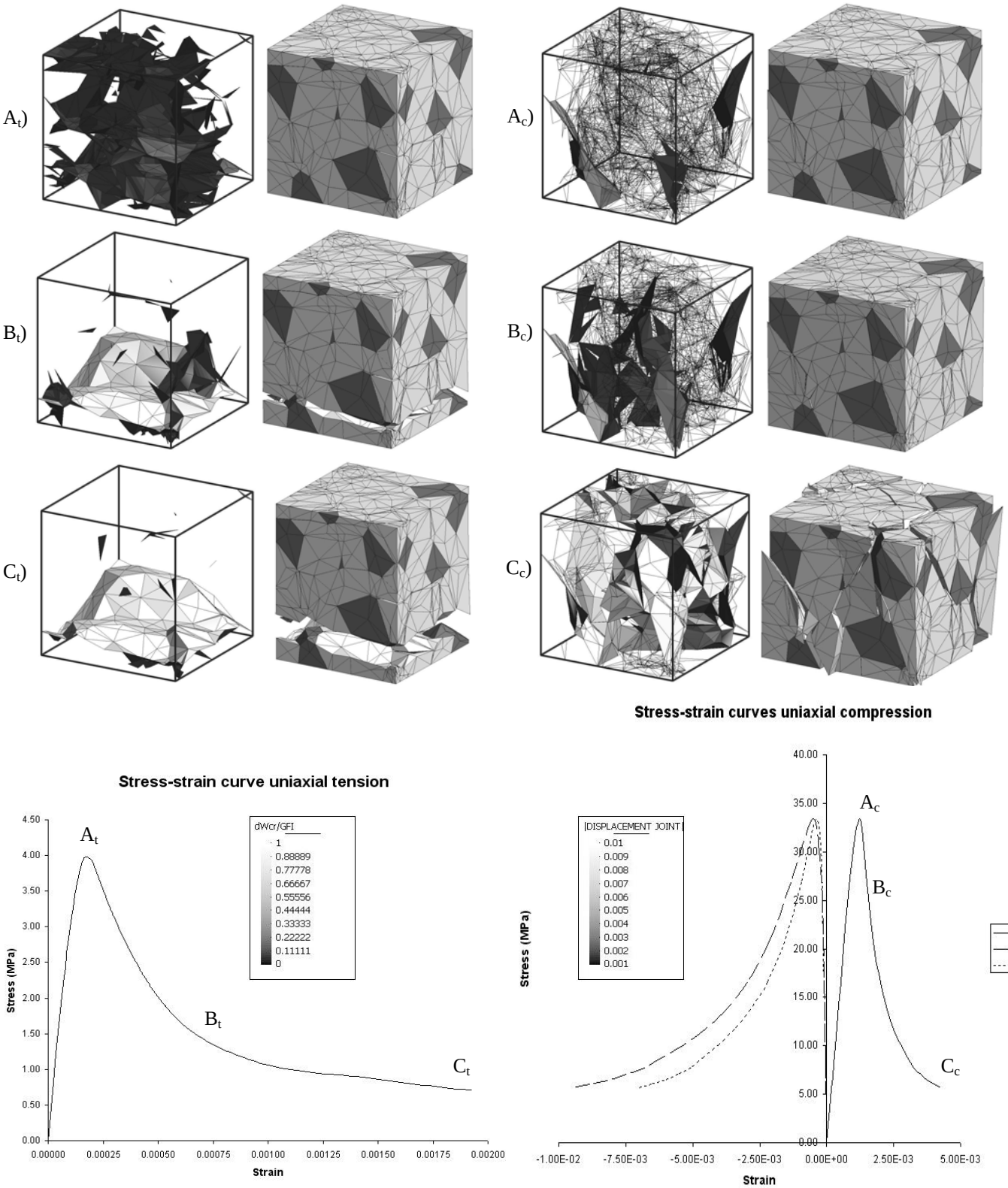

Fig. 2. Tension results: history parameter Wcr /G_F^I on cracked interfaces (1st column) and deformed shape (2nd column). Compression results: norm of relative displacements on cracked interfaces (3rd column) and deformed shape (4th column) at loading states A, B and C.

3.2 Results in uniaxial compression

Compression loading is also applied to the same 14-aggregate specimen. In this case the prescribed displacement is applied only to the nodes belonging to the continuum elements which have side faces sitting on the upper or lower platen, but not to the element tips or edges reaching those planes between adjacent interfaces. This relaxation of the boundary conditions, which tries to reflect the physical phenomenon of sharp tip or edge crushing against a steel load platen, is needed in order to obtain realistic crack patterns reaching the specimen boundary in the way shown in figure 2 (upper-right). Average stress-strain curves are represented at the bottom-right diagram of the figure. The horizontal semi-axes represent longitudinal (right) and transversal (left) strains. The detailed state of cracking and deformation for each of the four stress states A_c, B_c, C_c marked on the curves, are represented in detail in each horizontal row of the upper-right images. In the left column only those interfaces which are in a "plastic state" (opening) and also their displacement modulus has exceeded a fixed threshold (minimum value at displacement legend- scale) are depicted. In the right column, the deformed shapes of the specimen at the same load levels are depicted. It can be observed that the detailed states reflect quite well the localization phenomenon with a progressively increasing number of planes which exceed minimum displacement threshold, and how a limited number of well defined inclined (shear band-type) planes divide the specimen in a few pieces forming a mechanism of wedges sliding with friction.

4 CONCLUDING REMARKS

The approach for concrete fracture using interface elements previously developed in 2-D, is being successfully extended to 3-D. This extension is requiring an important effort for improving efficiency of the pre-processing, analysis and post-processing tools. A realistic representation of the stress-strain curves and of the crack patterns and evolution are obtained. In particular, it is reassuring to see how the localization process takes place spontaneously, leading from initially distributed micro-cracking to macro-cracks crossing the specimen, perpendicular to the applied load in tension, or inclined to about 60 degrees forming wedge mechanisms in compression. Also the macroscopic stress-strain curves show realistic features, and exhibit the right proportions of strength values and other characteristic parameters. Current work aims at the analysis of more representative geometries with larger number of aggregates, subject to a larger variety of loading situations.

ACKNOWLEDGEMENTS

The third author thanks MEC (Madrid) for his position funded under the "Ramón y Cajal" program. The research grant MAT2003-02481 also from MEC is greatfully acknowledged.

REFERENCES

[1] Carol, I., López C. M. y Roa, O., "Micromechanical analysis of quasi-brittle materials using fracture-based interface elements", Int. J. Numer. Meth. in Engrg. Vol 52, pp.193-215 (2001).

[2] Carol, I., Prat, P. C. y López, C. M., "A normal/shear cracking model. Application to discrete crack analysis", J. of Engineering Mechanics, 123, No 8, pp. 765-773 (1997).